

Impact of tropical cyclone development on the instability of South Asian High and the summer monsoon onset over Bay of Bengal

Guoxiong Wu · Suling Ren · Jianmin Xu ·
Dongxiao Wang · Qing Bao · Boqi Liu ·
Yimin Liu

Received: 23 July 2012 / Accepted: 3 April 2013 / Published online: 3 May 2013
© Springer-Verlag Berlin Heidelberg 2013

Abstract This paper analyzes the evolution of the South Asian High (SAH) during and after the development of tropical cyclone Neoguri over the South China Sea (SCS) in mid-April 2008, the formation of tropical storm Nargis over the Bay of Bengal (BOB) in late April, and the Asian summer monsoon onset, as well as their interrelationships. Numerical sensitivity experiments are conducted to explore the underlying mechanism responsible for these seasonal transitions in 2008. It is demonstrated that strong latent heating related with tropical cyclone activities over the SCS can enhance the development of the SAH aloft and generate zonal asymmetric potential vorticity (PV) forcing, with positive vorticity advection to its east and negative advection to its west. Following the decay of the tropical cyclone, this asymmetric forcing leads to instability

development of the SAH, presenting as a slowly westward-propagating Rossby wave accompanied by a westward shift of the high PV advection. A strong upper tropospheric divergence on the southwest of the SAH also shifts westward, while positive PV eddies are shed from the high PV advection and eventually arrives in the southern BOB. Such synoptic patterns provide favorable pumping conditions for local cyclonic vorticity to develop. The latent heating release from the cyclogenesis further intensifies the upper-layer divergence, and the lower and upper circulations become phase locked, leading to the explosive development of the tropical cyclone over the southern BOB. Consequently, a tropical storm is generated and the BOB summer monsoon commences.

Keywords Zonal asymmetric forcing · Tropical cyclone · Instability · South Asian High

G. Wu · S. Ren · Q. Bao · B. Liu · Y. Liu (✉)
State Key Lab of Atmospheric Sciences and Geophysical Fluid
Dynamics (LASG), Institute of Atmospheric Physics, Chinese
Academy of Sciences, Beijing 100029, China
e-mail: lym@lasg.iap.ac.cn

S. Ren · J. Xu
National Satellite Meteorological Center, China Meteorological
Administration, Beijing 100081, China

S. Ren
Graduate University of Chinese Academy of Sciences, Beijing
100049, China

D. Wang
State Key Laboratory of Tropical Oceanography, South China
Sea Institute of Oceanology, Chinese Academic of Sciences,
Guangzhou 510301, China

B. Liu
Key Laboratory of Meteorological Disaster of Ministry of
Education (KLME), Nanjing University of Information Science
and Technology, Nanjing 210044, China

1 Introduction

The onset of the Asian summer monsoon (ASM) usually is spread over more than 1 month, from the beginning of May to early June. It evolves in a sequence in which the Bay of Bengal (BOB) monsoon starts first at the beginning of May, followed by the South China Sea (SCS) monsoon in mid-May, and finally the Indian summer monsoon in early June (Wu and Zhang 1998; Zhang and Wu 1998, 1999; Xu and Chan 2001; Mao and Wu 2007). In the lower troposphere, the monsoon onset is often preceded by the development of a monsoon onset vortex (MOV) (Krishnamurti and Ramanathan 1982; Krishnamurti et al. 1981; Lau et al. 1998, 2000; Yan 2005; Wu et al. 2012). The northward movement of the onset vortex can lead to a break in the ridgeline of the subtropical anticyclone in the

lower troposphere over the eastern BOB and activate the India-Burma trough, resulting in the onset of BOB summer monsoon (He et al. 2002; Liu et al. 2002). Based on observational data analysis and numerical experiments, Liu et al. (2002) demonstrated that the strong latent heating during the BOB monsoon onset generates a Rossby wave train that later facilitates the subsequent onset of the SCS summer monsoon.

The establishment of the vertical easterly shear over South Asia is commonly used to signify the ASM onset since it is well linked to the upper layer divergence (Webster and Yang 1992; Mao et al. 2004). However, the underpinning dynamics is the asymmetric potential vorticity (PV) forcing associated with the instability development of the SAH. This is because the PV change in tropical area is mainly caused by the change in absolute vorticity, while the atmospheric vertical ascent is proportional to the vertical shear of absolute vorticity advection:

$$w \propto -\frac{\partial}{\partial z} (\vec{V} \cdot \nabla(f + \zeta))$$

In the upper troposphere, enhanced instability of SAH can help positive PV advection on the east and south flanks of the SAH along the prevailing northeasterly, whereas in the lower troposphere it is favorable for negative PV advection by the southwesterly that originates from South Hemisphere and crosses the South Asia latitudes via the Somali Jet. As a result, absolute vorticity advection increases rapidly with increasing height across the latitudes between 5° and 20°N accompanied with prevailing ascent, which is in favor of the development of monsoon rainfall. Meanwhile to maintain vorticity balance at a steady state, local absolute vorticity decreases with increased divergence in the upper troposphere in response to the enhanced positive PV advection. Upper tropospheric pumping is thus formed. In the lower troposphere however, the local decrease of absolute vorticity due to the negative PV advection must be balanced by the local generation of positive vorticity, leading to development of local convergence. When the upper-layer pumping is phase-locked with the lower layer convergence, explosive cyclogenesis can be triggered. In this regard, the “vertical easterly shear” can be considered as a synoptic manifestation of the dynamical asymmetric potential vorticity forcing, and the study on the unstable development of the SAH should help understanding the dynamical process of the ASM onset.

Hsu and Plumb (2000) investigated the mechanism for the instability development of the upper tropospheric anticyclone by using idealized experiments based on a shallow-water equation model. Their results showed that with sufficiently large asymmetric forcing, the forced anticyclone becomes unstable and periodically sheds eddy westward. Using a global primitive equation model, Liu et al. (2007) demonstrated that heating over the Tibetan

Plateau (TP) leads to a potential vorticity (PV) minimum aloft, and if it is sufficiently strong the anticyclone circulation becomes unstable, presenting a westward-propagating quasi-biweekly oscillation. Using the general circulation model SAMIL, Guo and Liu (2008) showed that the strong latent heating released from a tropical cyclone can significantly influence the development of the anticyclone in the upper troposphere over Asia, i.e., SAH, which expands eastward over the western Pacific and is accompanied with high PV eddies on its east that move toward the equator. Apparently strong convective latent heating in the tropics in summer can produce zonal asymmetric forcing in the subtropics and induce the instability development of the SAH.

Prior to the ASM onset, the SAH migrates to the Indochina Peninsula mainly due to the diabatic heating over South Asia (Liu et al. 2012). The latent heating of the convection over the Indochina Peninsula further contributes to the intensification of the SAH. Notice that the SAH and MOV are the two dominant synoptic systems before the ASM onset. The MOV is confined to the lower troposphere while the SAH is in the upper troposphere. The MOV is generated by the air-sea interaction over the BOB, where the thermal forcing of the Tibetan Plateau and surrounding oceans plays an important role (Wu et al. 2012). It is important to note that, although the thermal forcing of Tibetan Plateau and the land-sea thermal contrast across South Asia always exist prior to the ASM onset and favors the genesis of the MOV, the latter doesn't necessarily develop every year (Fig. 1 and Table 2 of Wu et al. (2012)). This implies that the climatologically mean thermal forcing in the lower troposphere alone is insufficient for the genesis of MOV and that its development requires extra forcing. Most studies of the aforementioned SAH instability that is associated with strong heating are focused on summertime. Can this instability occur in spring and whether this upper tropospheric process serves as such an extra forcing for the near-surface MOV development, hence jointly contribute to the monsoon onset? Such essential dynamic issues are not well addressed yet. In their case study of the year 1989 Asian monsoon onset, Wu and Zhang (1998) found that after the BOB and SCS monsoon onsets, the SAH is greatly intensified, and a very strong divergent region appears to the southwest of the SAH center and over the southwestern coast of the Indian subcontinent, right in between the southeasterly to its north and northeasterly to its south. This upper layer divergence acts as a strong air-pumping and contributes to the Indian monsoon onset in June. Whether this mechanism can be applied to the BOB monsoon onset in early May is another question that needs to be answered.

This study addresses above scientific questions by approach of both observational data analysis and numerical model simulations. Synoptic weather systems in 2008 provide an ideal case for this study. Before the BOB

Fig. 1 Tropical cyclone activities in 2008: **a** position at 00 UTC of tropical cyclone Neoguri over the SCS and Nargis over the BOB in late spring, **b** time series of average and gust wind speeds (m s^{-1}) as well as the surface pressure (hPa) recorded at Xisha Station ($112^{\circ}19'E$, $16^{\circ}51'N$), and the distribution of the total precipitation (mm) during the tropical cyclone activities of **c** Neoguri over the SCS (5° – $20^{\circ}N$; 110° – $120^{\circ}E$, *rectangle*) from April 13 to 19 and **d** Nargis over the BOB (5° – $20^{\circ}N$; 85° – $100^{\circ}E$, *rectangle*) from April 23 to May 4

monsoon onset in spring 2008, Typhoon Neoguri developed in the SCS while the SAH was abnormally intensified in the upper troposphere, followed by the development of the intense tropical storm Nargis over the BOB. Potential interactions between above systems are investigated and the underlying mechanism is explored in this study.

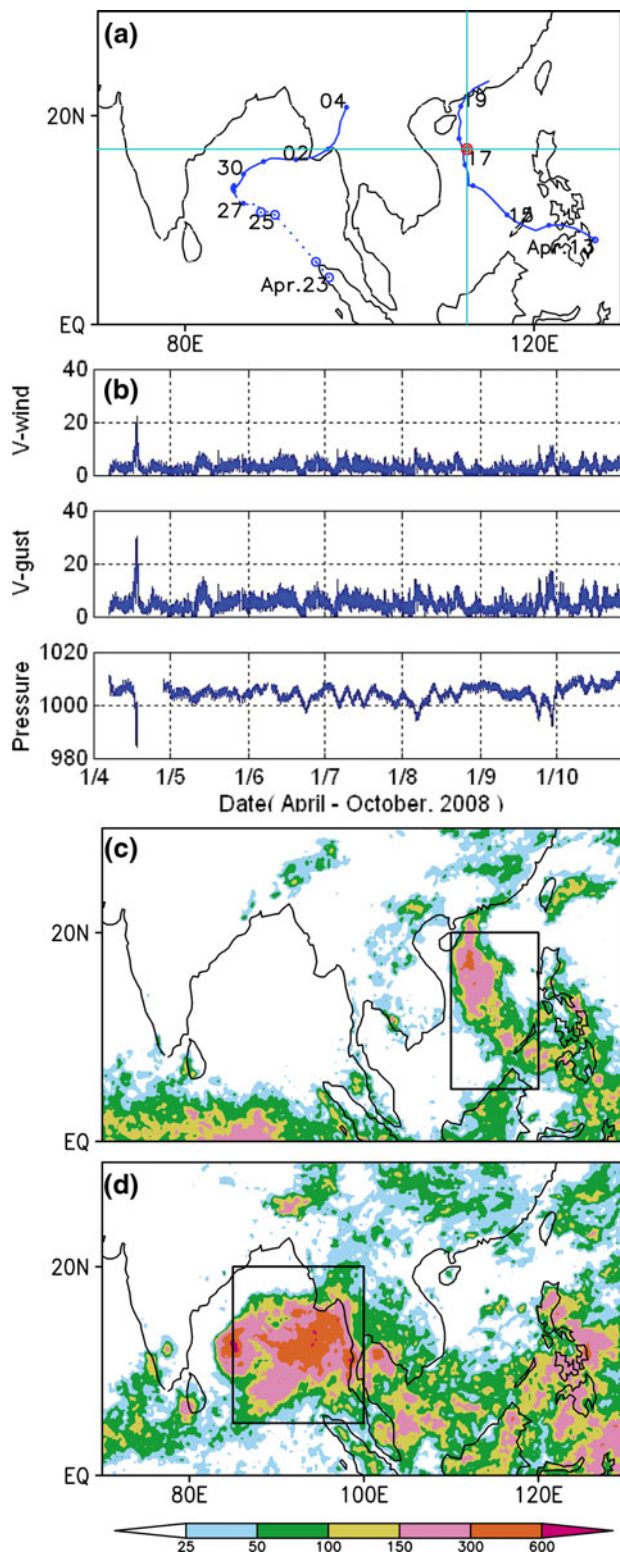
The study is organized as follows: The overview of the 2008 Asian summer monsoon onset based on observation is given in Sect. 2, which includes the tropical cyclone activity over the SCS, the zonal asymmetric PV forcing and subsequent evolution of the instability of the SAH, and the genesis of the tropical storm over the BOB and its growing to the more intense tropical storm Nargis. Section 3 gives a brief introduction to the general circulation model employed in this study as well as the experiment design. Experimental results are compared with observations in Sect. 4, with focus on the key issue of how the strong latent heating over the SCS in spring affects the unstable development of the SAH in the upper troposphere and the genesis of the tropical storm over the BOB, as well as the ASM onset. Conclusions and discussion are presented in Sect. 5.

2 Observational overview of the 2008 Asian summer monsoon onset

Two precipitation data sets are used in this study: (1) TRMM 3B42 (Huffman et al. 2007) dataset that includes 3-h precipitation rate at spatial resolution of 0.25° (longitude) \times 0.25° (latitude); (2) the daily precipitation records of the Global Precipitation Climatology Project (GPCP) at spatial resolution of 1° (longitude) \times 1° (latitude) (Huffman et al. 2001). Temperature, geopotential height, and wind vector are extracted from the National Center for Environmental Prediction (NCEP) reanalysis daily mean dataset (Kalnay et al. 1996) with spatial resolution of 2.5° (longitude) \times 2.5° (latitude). The tropical storm tracks are derived from the Joint Typhoon Warning Center (JTWC) Best Track dataset (Yu et al. 2007), which provides cyclone categories for the period after 2000.

2.1 Tropical cyclone activity and the Asian summer monsoon onset

The tropical cyclone Neoguri developed over the SCS (Fig. 1a) from 14 to 19 April 2008. Neoguri is the first



tropical storm and the earliest one invading China in the 2008 Pacific typhoon season. It formed on April 13 from a low pressure disturbance in the east of the island of Mindanao in the Philippines. After crossing the island on April

14, it intensified into a tropical depression (TD) over the SCS and a tropical storm on April 15, finally attained typhoon status on April 16 and moved northward. The typhoon reached its peak intensity on April 18 as it approached the island of Hainan, but weakened after landing in South China on April 19 before it died down. During the life cycle of Neoguri the highest 10-min sustained wind was 150 km/h (90 mph), the highest 1-min sustained wind was 185 km/h (115 mph), and the lowest pressure was 950 hPa. The local barograph and anemograph at the Xisha Marine Research Station (112°19'E, 16°51'N), which is close to the typhoon track as shown in Fig. 1a, recorded the passage of the typhoon between April 17 and 18 (Fig. 1b). The time-mean and gust wind speed exceed 20 and 30 m s⁻¹ respectively, and the surface pressure is below 990 hPa (Long et al. 2010). The total precipitation retrieved from the TRMM (Fig. 1c) shows a heavy rainfall belt with more than 150 mm over the SCS region (10°–20°N; 110°–120°E) during 13–19 April 2008. The total precipitation exceeded 300 mm over the northern SCS. Such a heavy precipitation implies the latent heating over the SCS was very strong in mid-April of 2008.

After Typhoon Neoguri passed over the SCS, another deep convection activity started in the southeastern BOB since April 19 and gradually became organized and consolidated. By April 23 (Fig. 1a), a local low-pressure center was formed and later developed into a well-defined TD on April 25 as it moved northwestward (Kikuchi et al. 2009). On April 27, the system intensified into tropical storm Nargis. On April 28, it was upgraded to a severe tropical storm and further developed to a very severe tropical storm by April 29 due to northward water vapor transport (Li et al. 2012). On May 2, Nargis reached its peak intensity and landed on the western coast of Myanmar. The total precipitation over most of the BOB was more than 150 mm and exceeded 600 mm in some places (Fig. 1d), bringing severe damage to the area.

The Webster and Yang monsoon index, which is defined as the vertical shear of zonal wind between 850 and 200 hPa (Webster and Yang 1992), and the Mao monsoon index, which is defined as the meridional gradient of middle- to upper-level temperatures averaged between 200 and 500 hPa (Mao et al. 2002) are used to determine the BOB and SCS summer monsoon onset date. Here BOB covers the area between 5° and 20°N and 85°–100°E while the SCS covers area between 5° and 20°N and 110°–120°E, as indicated by the two boxes in Fig. 1c, d respectively. Results show that based on the Mao/Webster-Yang index, the 2008 BOB summer monsoon onset occurred on April 25/24 and the SCS summer monsoon onset on May 1/April 30 (Fig. 2a, b). The

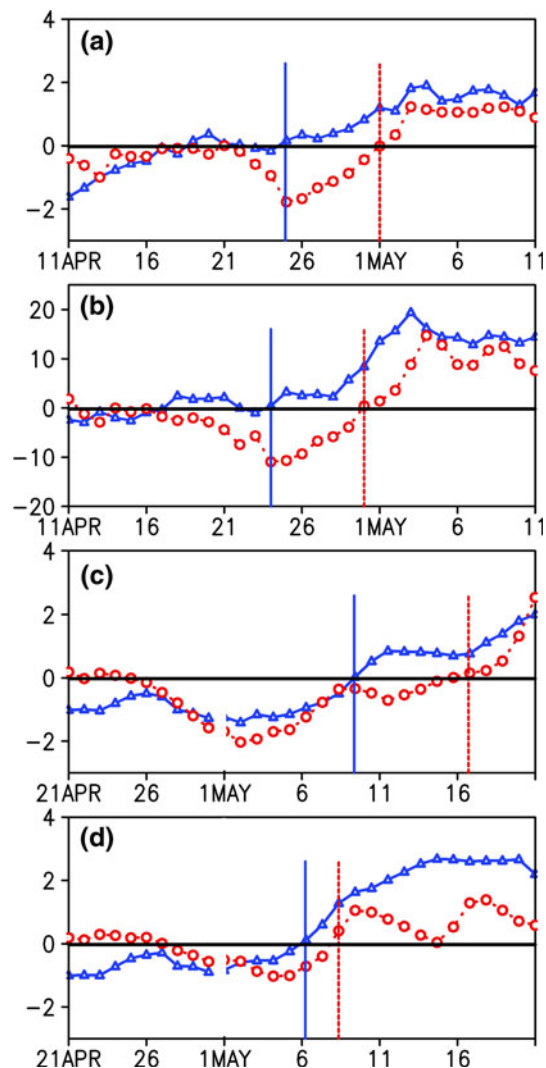


Fig. 2 Time series of the summer monsoon index based on the reanalysis for 2008 **a** calculated by method of Mao et al. (2002), **b** calculated by definition of Webster and Yang (1992). The summer monsoon index based on model results and by the method of Mao et al. are shown in **c** the control experiment CTL and **d** the latent heating experiment HTG. The *dashed red curve* is for the SCS (5–20°N; 110–120°E) summer monsoon index, and the *solid blue curve* for the BOB (5–20°N; 85–100°E) summer monsoon index. Unit is K for **a**, **c**, and **d**; and m s⁻¹ for **b**

monsoon onset dates in these two regions determined by the Webster and Yang index are only 1 day earlier than those defined by Mao's monsoon index, indicating a consistency between the two indexes. Compared with the climatological mean BOB monsoon onset on May 5/1 and the SCS monsoon onset on May 13/12 based on the Mao/Webster-Yang index, the BOB and SCS monsoon onsets in 2008 commenced earlier by about one to two pentads and two to three pentads, respectively. Note that the BOB monsoon onset occurred about 1 week after the SCS tropical cyclone Neoguri had died away.

2.2 Evolution of the SAH and the associated planetary vorticity advection

Figure 3 shows the development of the geopotential height, stream field, and planetary vorticity advection ($-\beta v$) at 200 hPa during and after Typhoon Neoguri activities over the SCS. From April 13 to 19 when Neoguri was developing and moving northward, the geopotential height of the SAH increased from about 12440 to 12460 gpm while the anticyclone center shifted northwestward from the northwest Pacific on April 13 to the Indochina Peninsula on April 19 (Fig. 3a–d). By April 19, the 12460 gpm contour of the SAH had reached the eastern BOB and South China (Fig. 3d). Consequently, a well-organized pattern of planetary vorticity advection that was positive to the east of the SAH and negative to its west appeared, forming a zonal asymmetric vorticity forcing on the atmosphere.

The development and northwestward movement of the SAH during the evolution of Neoguri can be explained qualitatively in terms of the inhomogeneous diabatic heating in both the vertical and horizontal. The change in vertical vorticity due to an imposed diabatic heating Q can be expressed as (Wu and Liu 1999):

$$\frac{\partial \zeta_z}{\partial t} \propto \frac{1}{\theta_z} \vec{\zeta}_a \cdot \nabla Q, \quad \theta_z \neq 0 \tag{1}$$

where ζ_z is the vertical component of relative vorticity, $\vec{\zeta}_a$ is absolute vorticity, and the other symbols are conventional variables in meteorology. Within the tropical heating region, the vertical differential heating usually is dominant (Wu et al. 2004), i.e.,

$$\frac{\partial \zeta_z}{\partial t} \propto \frac{1}{\theta_z} (f + \zeta_z) \frac{\partial Q}{\partial z}, \quad \theta_z \neq 0 \tag{2}$$

At levels above the convective heating maximum within Neoguri where $\partial Q / \partial z < 0$, an anticyclone will develop locally, leading to the intensification of the SAH. On the other hand, outside the latent heating domain where $\partial Q / \partial z = 0$, the change in vertical vorticity is mainly due to the correlation in horizontal gradients between temperature and diabatic heating (Liu et al. 2001):

$$\frac{\partial \zeta_z}{\partial t} \propto -\frac{g}{f\theta\theta_z} (\nabla_h \theta \cdot \nabla_h Q), \quad \theta_z \neq 0 \tag{3}$$

where ∇_h denotes horizontal gradient. Because of the local latent heating induced warm-core structure of the convective system, the associated horizontal temperature gradient is inward. Thus on the north of the tropical convection, the horizontal temperature gradients of both the large-scale environment and the convection system are positively correlated with the horizontal heating gradient, which, according to (3), induces negative vorticity and positive

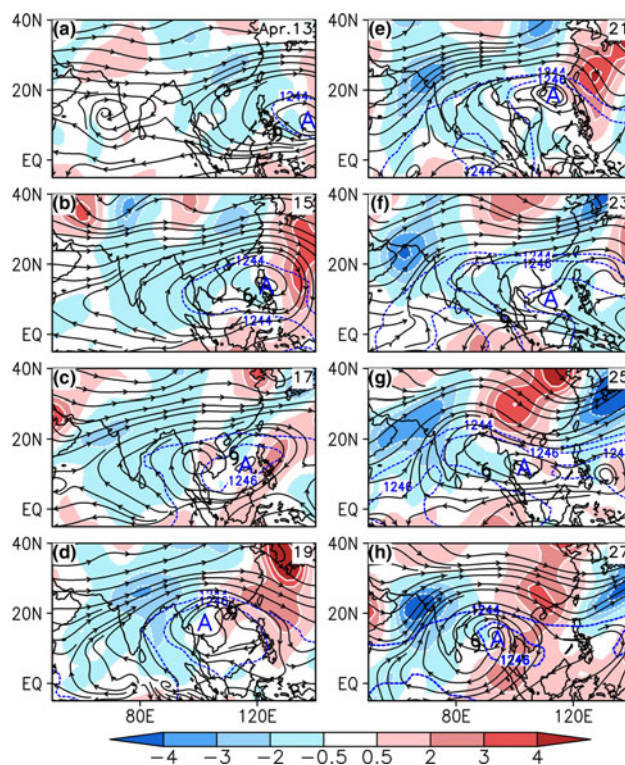


Fig. 3 The 200-hPa geopotential height (dashed blue contour, unit is 10 gpm), wind stream and planetary vorticity advection (shading, unit is 10^{-10} s^{-2}) during 13–27 April 2008. The symbol “S” in a–d indicates the location of Neoguri, and in f, g, and h indicates the location of the tropical cyclone over the BOB, and “A” is the center of the anticyclone

geopotential height to the north of the heating. Hence the latent heating released from Neoguri can enhance the SAH above and contribute to its northward movement in the upper troposphere, as demonstrated in Fig. 3a–d.

The aforementioned zonal asymmetric planetary vorticity advection can trigger the unstable development of the SAH and result in its northwestward movement, as demonstrated in Fig. 3a–d. After Neoguri made landfall in South China on April 19 and then decayed, the SAH center and the ridge of the geopotential high to its north started to propagate eastward along the westerly flow (Fig. 3e–f). After April 21, another ridge–trough system developed along the subtropical westerly over North China. As the ridge developed, negative (positive) potential vorticity advections behind (in front of) the ridge increased and the center of the SAH in the tropics moved westward again. By April 25 (Fig. 3g), the ridge was located along 90°E, while the trough was located over the eastern coast of China. The strong northwesterly in front of the ridge was accompanied by strong positive vorticity forcing and dominated most of eastern China. On April 27 (Fig. 3h), a noticeable northerly developed on the east of the closed 12460 gpm contour that covered

the Andaman Sea and the Gulf of Thailand. The zonal asymmetric vorticity forcing was further enhanced and the positive vorticity advection became dominant over the southern BOB region, contributing to the development of vertical ascent there.

2.3 Zonal asymmetric potential vorticity forcing

Figure 4 shows the evolution during the BOB monsoon onset of the potential vorticity ($P = \alpha(f + \zeta)\partial\theta/\partial z$) distribution at the 360-K isentropic surface, which is close to the tropopause in the subtropics (Hoskins et al. 1985). On April 19 (Fig. 4a), when Neoguri arrived in South China and started to decay, it left behind a negative PV minimum center in the upper troposphere just over the SCS, with a southward advection of high PV appearing to its northeast over the eastern coast of China. As the PV minimum moved northeastward by April 21 (Fig. 4b), the high PV “trough” in front of the PV minimum was intensified and extended southwestward, with its southern front arriving at the eastern coast of the Philippines. High PV eddies were shed from the trough and traveled westward along the tropical easterly, forming a zonal high PV belt extending from the Philippines to the eastern BOB. The shed high PV eddies continued to travel westward until April 23 (Fig. 4c) with the westernmost enclosed center reaching the southeastern BOB, favoring local cyclone system development in the lower troposphere (Fig. 1a).

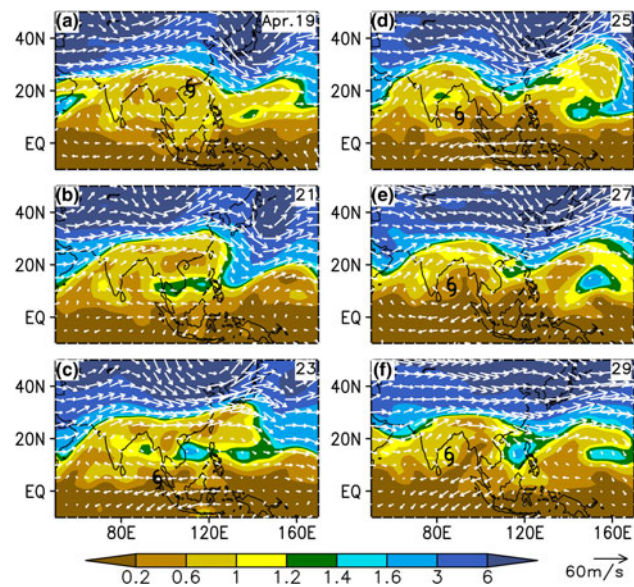


Fig. 4 Wind (vector, unit is m s^{-1}) and potential vorticity (shading, unit is $\text{PVU} = 10^{-6} \text{ m}^2 \text{ s}^{-1} \text{ K kg}^{-1}$) at the 360-K isentropic surface during 19–29 April 2008, after the occurrence of Typhoon Neoguri. “6” indicates the location of the tropical cyclone

2.4 Genesis of the BOB tropical cyclone Nargis

Accompanied by the northwestward migration of the SAH during the development of tropical cyclone Neoguri over the SCS (Fig. 3), upper-layer divergence associated with the negative velocity potential appeared to the southwest of the SAH just above the southern BOB (Fig. 5a–c). After Neoguri decayed on April 19, the SAH continued to move westward (Fig. 3) and the high PV eddies were continuously shed from the high PV trough over the western Pacific and then propagated westward (Fig. 4a–c). Meanwhile the upper tropospheric negative velocity potential and divergence over the southeastern BOB were enhanced (Fig. 5d, e). By April 23, the velocity potential increased to $-6 \times 10^{-6} \text{ m}^2 \text{ s}^{-1}$ and the divergence was intensified remarkably to $1.5 \times 10^{-5} \text{ s}^{-1}$, in accordance with the newborn MOV there (Fig. 5f). This newborn MOV led to the BOB monsoon onset 2 days later on 25th before it developed into the disastrous tropical storm Nargis on 27th (Fig. 5h).

The circulation evolution in the lower troposphere demonstrates that the genesis of the tropical depression on April 23 was also associated with the cold outbreak in southern China. Mao and Wu (2011) have shown that during April 22–24, a large-scale horizontal shear flow

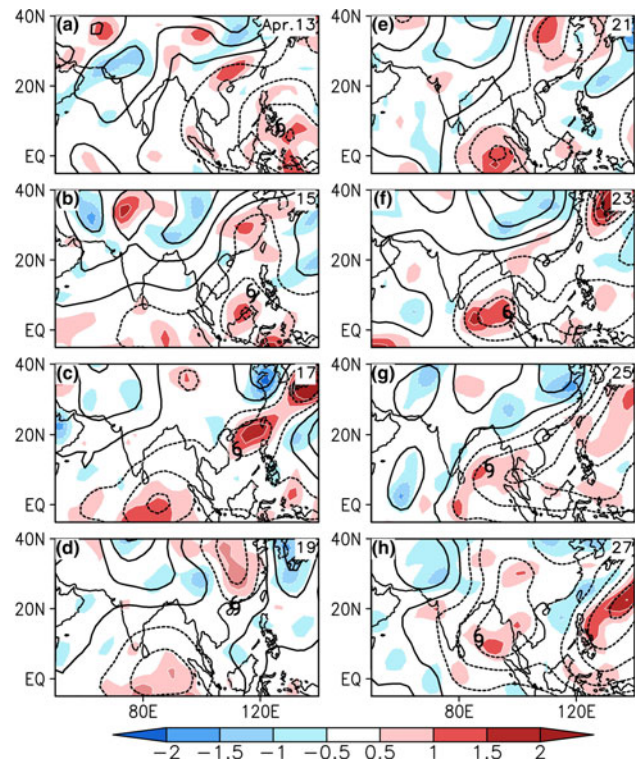


Fig. 5 The 200-hPa divergence (shading, unit is 10^{-5} s^{-1}) and velocity potential during 13–27 April 2008 (dashed curve for negative, solid curve for positive, interval is $2 \times 10^{-6} \text{ m}^2 \text{ s}^{-1}$). “6” indicates the location of the tropical cyclone

formed between strong equatorial westerlies and tropical-subtropical easterlies over the southern BOB. This barotropically unstable zonal flow eventually induced the development of Nargis. Since the equatorial westerlies existed before the formation of Nargis, the development of the tropical-subtropical easterlies should have played an important role in the genesis of Nargis. Figure 6a, b show the distributions of geopotential height and wind at 850 hPa. On April 21 (Fig. 6a), there was an apparent westerly along the equator but there was no easterly to its north. From April 22 onward (Fig. 6b) a high-pressure system spread southeastward from central China with its intensity gradually increased. Corresponding to the lower-level anticyclone development, the air temperature at 850 hPa decreased by -2 to -4 K from April 22 to 23 over South China (Fig. 6c). Influence of the cold air could reach the eastern BOB and the Indochina Peninsula, where a 2 K-drop in temperature was observed. This cold outbreak can be seen more clearly from the vertical cross section of temperature and circulation along 115°E on April 23 (Fig. 6d). An evident cold front with a surface temperature gradient of 5 K per 10° latitude was located in South China, with its front reaching the SCS. To the south of the high pressure, an easterly belt developed rapidly and extended westward across the central BOB (Fig. 6b). Barotropic unstable shear flow formed between the easterly and the equatorial westerly, which is favorable for the formation of the tropical depression and its subsequent intensification.

The strong cold outbreak on April 23 not only contributed to the formation of the MOV over the southeastern BOB, but also brought significant changes to synoptic circulation. As indicated in Fig. 3, the SAH continued to move westward due to its unstable development. Consequently the geopotential height at 200 hPa over Asia changed from being low in the west and high in the east before April 23 to a reversed configuration afterward. As a result, areas with strong positive planetary vorticity advection to the east of the SAH continued to expand southward. By April 27, when this positive vorticity advection reached the equator, the SAH center was located just above the eastern BOB (Fig. 3h). In association with the highly dispersed spiral-shaped streamline to the west of the center, a noticeable and very well-organized divergence center stronger than $1.5 \times 10^{-5} \text{ s}^{-1}$ developed over the central BOB at 200 hPa (Fig. 5g, h), again forming a strong upper-troposphere pumping. These factors, combined with the unstable background flow in the lower troposphere and the favorable oceanic conditions during mid to late April 2008 (McPhaden et al. 2009), provided ideal conditions for the tropical cyclone to develop rapidly into severe tropical storm Nargis on April 27, as demonstrated in Fig. 1a.

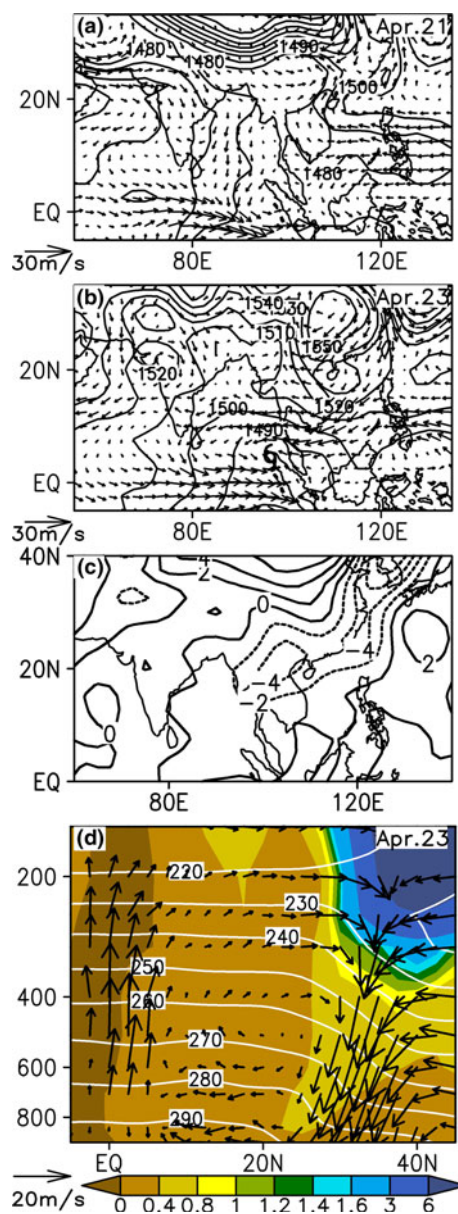


Fig. 6 Distributions at 850 hPa of wind (vector, unit is m s^{-1}) and geopotential height (contour, interval is 10 gpm) on **a** April 21 and **b** April 23, and **c** the temperature tendency between April 23 and April 22 (unit is K days^{-1}), **d** the vertical cross section along 115°E of the wind vector (v in m s^{-1} and $-\omega$ in $10^{-2} \times \text{Pa s}^{-1}$), temperature (contour, unit is K), and potential vorticity (shading, unit is PVU) on April 23, 2008

As usual (e.g. He et al. 2002; Liu et al. 2002; Wu et al. 2012), the development of the MOV on 23rd led to the BOB monsoon onset on 25th by changing the large-scale circulation and bringing intense rainfall over the eastern BOB and Indochina Peninsula (Fig. 7). Before the monsoon onset, the ridgeline of the subtropical anticyclone at 850 hPa was located between 15 and 20°N , and the tropical easterly separated the subtropical westerly to its north from the equatorial westerly to its south (Fig. 7a–c). As the

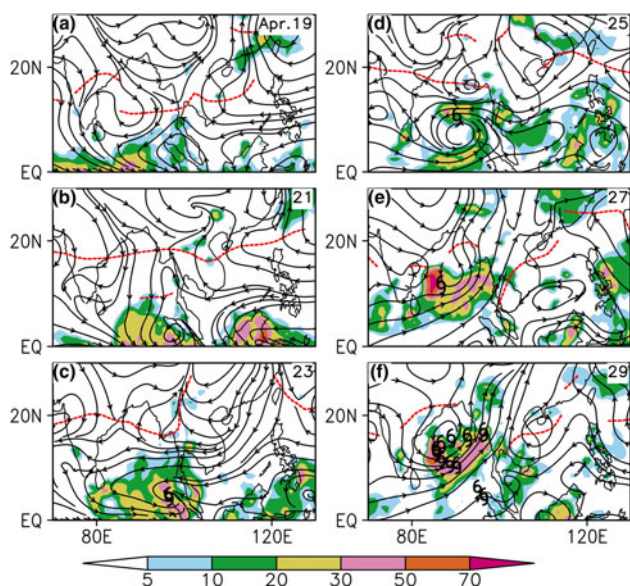


Fig. 7 The same as Fig. 4 except that the figure shows the distributions of streamline at 850 hPa and rainfall (shading, unit is mm days^{-1}). Red dotted curve indicates the ridgeline of the subtropical anticyclone. The symbol “6” in f shows the daily position of the typhoon along its track

MOV developed over the southeastern BOB (Fig. 7c) and migrated rapidly northward, the ridgeline as well as the tropical easterly belt got broken. The vortex was tied to the trough which was located to the south of the Tibetan Plateau, forming a deep trough over the central BOB (Fig. 7c–e). Strong southwesterly developed along the east side of the trough-vortex system while the equatorial westerly started to join with the subtropical westerly. This synoptic circulation pattern helped moving plenty of moisture from the BOB to Indochina Peninsula and South China, resulting in heavy precipitation and onset of the BOB summer monsoon (Fig. 7d–f). Above diagnoses clearly indicate that the earlier BOB monsoon onset in 2008 is to a great extent attributed to the development of the tropical storm Nargis.

3 Model description and numerical experiment design

Above diagnostic analysis indicates that the tropical cyclone developed over the BOB from April 23 to May 2 in 2008 was derived from MOV, which was generated 1–2 days before the BOB monsoon onset. The formation of this tropical storm and its rapid intensification into the severe tropical storm Nargis were strongly influenced by unstable development of circulation in the upper troposphere. In addition, the strong cold outbreak from South China also made great contribution to the intensification of the tropical cyclone after BOB monsoon onset. In fact, there were distinct features of circulation evolution before

the BOB monsoon onset in 2008: (1) the strengthening and northwestward movement of the SAH in spring was closely associated with the development of tropical cyclone Nargis over the SCS; (2) An upper-level divergence center was formed right over the southern BOB, accompanied by westward propagation of the unstable SAH after Nargis died out; (3) the zonal asymmetric PV forcing associated with the unstable development of the SAH produced a phase-lock with the lower tropospheric barotropic or baroclinic unstable circulation and triggered the development of a MOV, which finally led to the Asian monsoon onset. To further investigate whether above features are unique in 2008 or whether they are more general and instructive for the ASM onset, sensitivity experiments by global model are conducted.

3.1 Model description and experiment design

The model used for this study is the Flexible Global Ocean-Atmosphere-Land System model (FGOALS2) developed at LASG/IAP (Bao et al. 2010b). The atmospheric component of FGOALS is the Spectral Atmospheric Model of IAP/LASG (SAMIL). Its horizontal resolution is rhomboidal-truncated at wave number 42 with approximately $2.81^\circ\text{longitude} \times 1.67^\circ\text{latitude}$ transformed grid. There are 26 levels in a $\sigma - P$ hybrid coordinate in the vertical (Wang et al. 2005). The cumulus parameterization scheme was developed by Tiedtke (1989). Previous studies have shown that SAMIL can realistically simulate the ASM onset (Bao et al. 2010a).

In control run (CTL), sea surface temperature (SST) is prescribed based on monthly average Hurrell-modified Hadley SST from 1949 to 2001 (Hurrell et al. 2008), which is then linearly interpolated into the model dates. The model is initialized at 0000 UTC 1 January and integrated till the end of July. Initial fields are derived from the NCEP climatological means.

The sensitivity run (hereafter HTG) is the same as the CTL run except that convective heating is inserted into the SCS region from April 21 to 30. April 21 is selected as the beginning time for imposing the forcing, about 1 week later than the birth of Nargis on April 13 (Fig. 1a). This is because the BOB summer monsoon onset date in the CTL run is on May 9 (Fig. 2c), which is about 1 week later than the observation on May 2 (Mao et al. 2002). To separate the effect of the SAH unstable development from the air-sea interaction on the genesis of the MOV over the southern BOB, the same SST is used for both the CTL and HTG experiments to minimize the difference in air-sea interaction between the two experiments. To mimic Nargis’s heating distribution, its thermal status in the troposphere is first analyzed. Figure 8a shows a cross section of the distribution of temperature deviation from

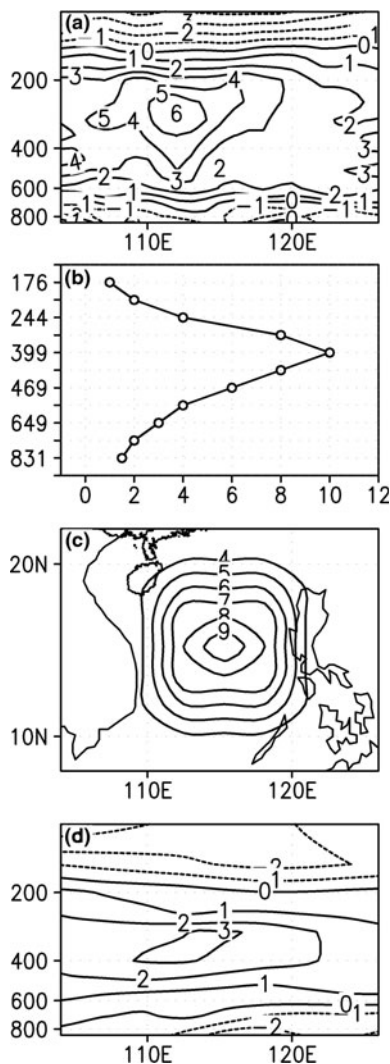


Fig. 8 **a** Vertical cross section of the zonal deviation temperature across the center of tropical cyclone Neoguri (17.1°N) as observed on April 17; **b** the imposed vertical latent heating profile at the heating center (115°E, 15°N) and **c** horizontal distribution of the latent heating at the maximum heating level near 350 hPa, which was added into the model in the HTG experiment; and **d** the cross section of the zonal deviation temperature in the HTG experiment along 15°N on April 27. Unit is K in **a** and **d**, and K days⁻¹ in **b** and **c**

the zonal mean along 17.1°N on April 17. A warming center with up to 6 K higher temperature is located at 112°E near 300 hPa. Accordingly, an idealized heating distribution as shown in Fig. 8b–d is designed. A maximum heating rate of 10 K days⁻¹ is located at the tenth model level (about 350 hPa) and at 115°E, 15°N while it decreases upward, downward, and outward (Fig. 8b, c). The heating region is confined to the SCS area bounded by 110°–120°E and 10°–20°N. Such a prescribed three-dimensional heating pattern is then added to the thermodynamic equation of the model from April 21 to 30. The cross section of the zonal deviated temperature in the HTG

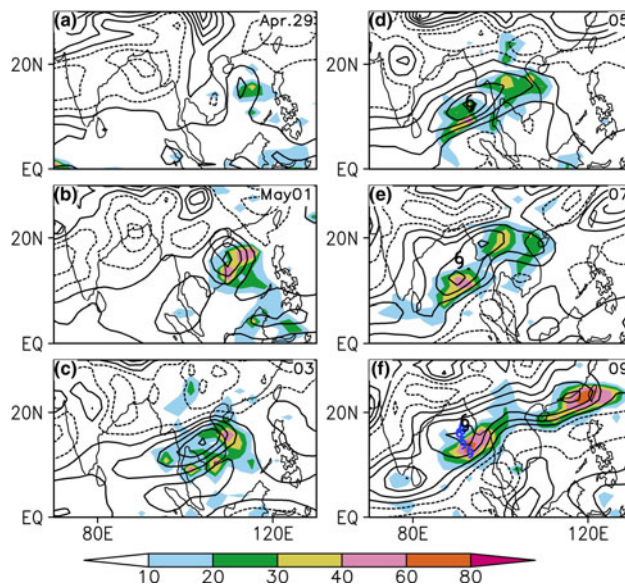


Fig. 9 Precipitation (shading, unit is mm days⁻¹) and vertical vorticity at 700 hPa (contour, interval is $1 \times 10^{-5} \text{ s}^{-1}$) for every other day from **a** April 29 to **f** May 9 in the heating experiment HTG. “6” indicates the location (**d**, **e**) and track (**f**) of the tropical cyclone generated in the HTG experiment

run along 15°N on April 27 is presented in Fig. 8d, which shows that a weaker warming center of 3 K is generated at 112°E near 350 hPa, fairly close to the warming center in the observation as shown in Fig. 8a. By comparing the differences between the model outputs of the CTL and HTG experiments, the impacts of the springtime tropical cyclone over the SCS on the unstable development of the SAH and the BOB monsoon onset can be evaluated.

3.2 Summer monsoon onset date

The monsoon onset index of Mao et al. (2002) is used to define the onset date. In the CTL run, the BOB and SCS summer monsoon onset dates are May 9 and 15 respectively (Fig. 2c). While the simulated SCS monsoon onset date is close to the observed date of May 18 (Mao et al. 2002), the simulated BOB monsoon onset date is about 1 week later than the observed date of May 2. In the HTG run, the BOB and SCS summer monsoon onset dates are May 6 and May 8 respectively (Fig. 2d). The fact that the strong convection heating over the SCS can trigger earlier monsoon onsets over the BOB and SCS regions is well simulated and agrees with what was observed in 2008. However, the CTL run failed to simulate the formation of the tropical cyclone over the BOB (figures not shown). This result shows that the climatological mean condition is insufficient for generation of MOV, whose development requires extra forcing. In contrast, HTG result demonstrates

that the imposed convective heating over the SCS can generate a vortex with behavior similar to that observed for Nargis. Consequently, the summer monsoon intensity simulated by HTG noticeably increases in the early days after the monsoon onset compared to that of the CTL run. Hereafter we will concentrate on how the strong diabatic heating over the SCS can initiate a MOV over the BOB and finally leads to the ASM onset.

4 Effects of SCS convective heating on ASM onset

HTG results show that a local cyclonic circulation in the lower troposphere gradually grows with increased precipitation after convective heating is introduced over the SCS on April 21. By April 29 (Fig. 9a), a distinct positive vorticity is generated at 700 hPa with intense precipitation of more than 30 mm days^{-1} occurring to its southeast.

When the imposed external latent heating is discontinued on April 30 this cyclone starts to propagate westward, accompanied by increasing precipitation (Fig. 9b, c). On May 5 a remarkable cyclogenesis appears over the eastern BOB (Fig. 9d), which has intense surface mean wind of 12 m s^{-1} and becomes a tropical storm just 1 day before the simulated BOB monsoon onset (Fig. 2d). It is therefore regarded as MOV. From May 7 to May 9, this newborn tropical storm moves northwestward—northeastward and results in torrential rains of over 60 mm days^{-1} to the west of the Peninsula (Fig. 9e, f). The entire process resembles

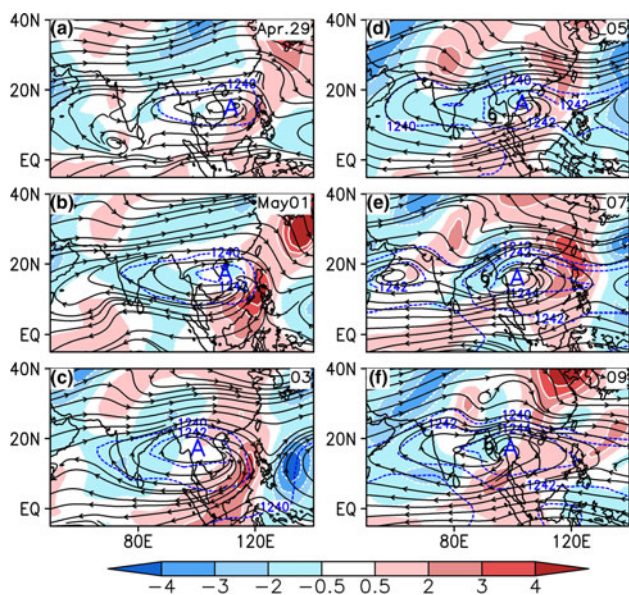


Fig. 10 The same as Fig. 9 except that this figure shows the distributions of the 200-hPa geopotential height (dashed blue curve, unit is 10 gpm), wind stream and planetary vorticity advection (shading, unit is 10^{-10} s^{-2})

fairly closely the observed evolution of the BOB tropical cyclone in 2008.

In the upper troposphere at 200 hPa, after the latent heating is imposed over the SCS in HTG, an obvious anticyclone develops over the SCS, which later becomes the SAH. The heating also induces a positive geopotential height tendency above the heating level and to its north. On April 29 HTG results show that the 12400-gpm contour has extended to South China in the north and to the BOB in the west (Fig. 10a), whereas in the CTL run it barely reaches the northern SCS (figure not shown). After the prescribed latent heating is removed, the HTG simulated anticyclone center at 200 hPa shifts westward systematically from the SCS to the Indochina Peninsula (Fig. 10b–d). On the east/west side of the anticyclone there exists northerly/southerly accompanied by positive/negative planetary vorticity advection, which contributes to the unstable development of the SAH and its westward movement. On May 5 (Fig. 10d), the center of the anticyclone moves to the Indochina Peninsula and strong divergent flow developed (Fig. 12d) over the southeastern BOB, where the surface tropical storm forms (Fig. 9d). Associated with the intensification of the tropical storm on May 7 and May 9 (Fig. 10e, f), the SAH develops and moves farther westward, leaving a strong divergence area just over the coastal ocean to the west of Myanmar (Fig. 12f), which is in a phase lock with the rapid intensification of the storm in the lower troposphere (Fig. 9e, f).

Figure 11 demonstrates the evolution of the PV and wind field at the 360-K isentropic surface. A belt of strong

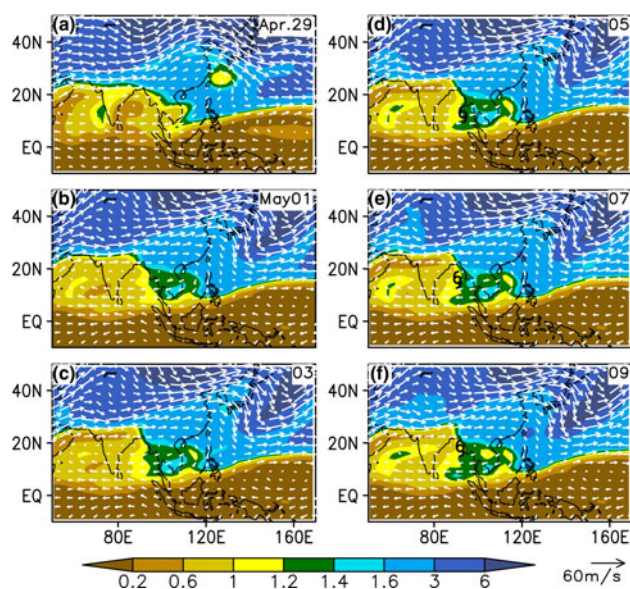


Fig. 11 The same as Fig. 9 except that this figure shows the distributions of wind (vector, unit is m s^{-1}) and potential vorticity (shading, unit is PVU) at the 360-K isentropic surface

PV gradient between 1.0 and 1.6 PVU is meandering between the tropics and subtropics, indicating the location of the tropopause. The imposed convective heating in the SCS produces a gradually increasing PV minimum just above the heating region at the 360-K surface. By the end of the imposed heating, the PV minimum over the SCS is less than 1.2 PVU, and a ridge of minimum PV extends over eastern China (Fig. 11a). Meanwhile there appears another low PV in the tropics from the Arabian Sea to the Indian subcontinent. After the imposed heating is discontinued, the low PV ridge of 1.6 PVU over China starts to move eastward, leading to a southwestward high PV advection on its eastern front over the northwest Pacific, whereas the low PV over India also develops and extends northeastward (Fig. 11b). The pattern of southwestward advection of high PV over the western Pacific and the northeastward advection of low PV over India persists for a while (Fig. 11c). On May 5 a high PV tongue of more than 1.2 PVU appears just above the southeastern BOB (Fig. 11d), in conjunction with the BOB tropical storm formation and development (Fig. 9d). After the BOB monsoon onset on May 6, high PV eddies continue to shed from the high PV trough (Fig. 11e, f) while the tropical storm in the lower troposphere continues to develop, resulting in severe weather over the western Peninsula (Fig. 9f).

In association with the unstable development of the SAH at 200 hPa and the southwestward advection of the

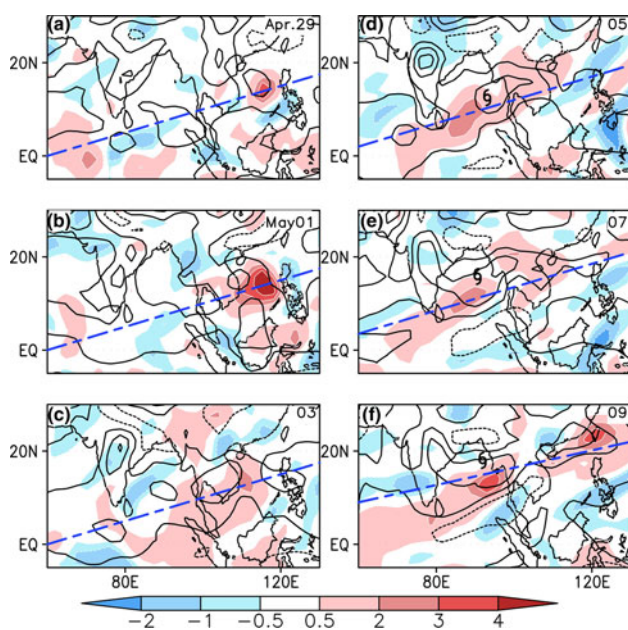
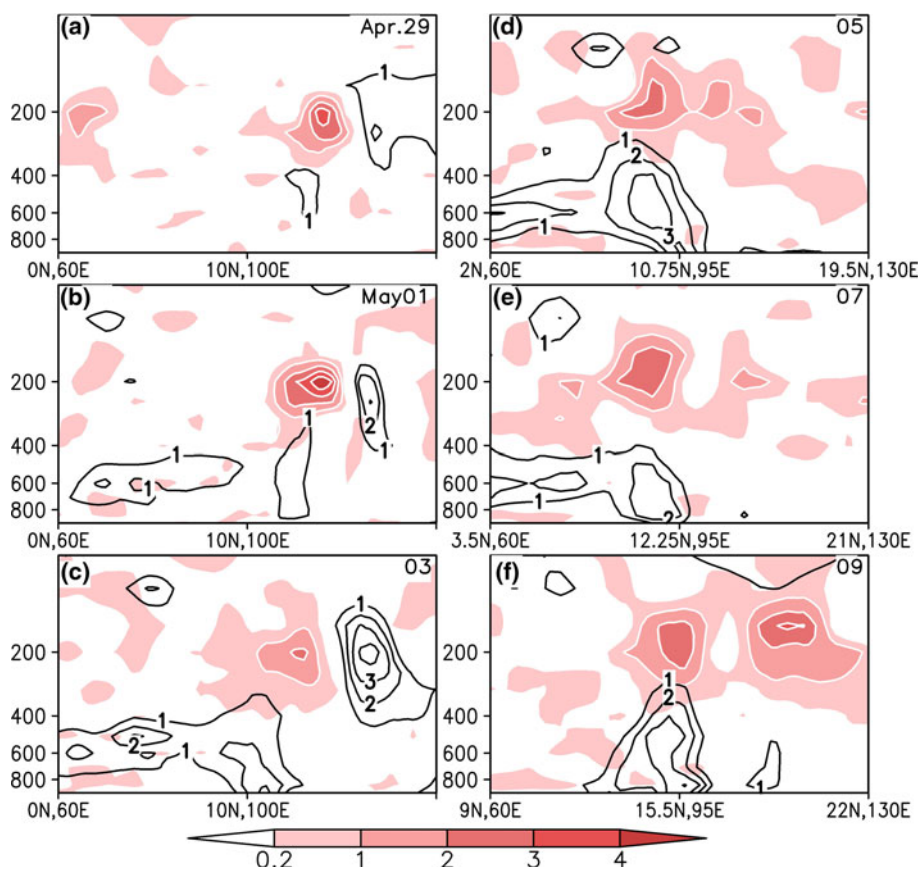


Fig. 12 The same as Fig. 9 except that this figure shows the distributions of the 200-hPa divergence (shading, unit is 10^{-5} s^{-1}) and 850-hPa vertical vorticity (contour, dotted for negative, interval is $2 \times 10^{-5} \text{ s}^{-1}$). The dashed blue lines indicate the orientation along which the cross section in Fig. 13 is plotted

high PV at the 360-K isentropic surface, the divergence center at 200 hPa, which was induced by the imposed convective heating over the SCS, also gradually propagates southwestward (Fig. 12). Along its path across the Indochina Peninsula, its intensity decreases from higher than $4.0 \times 10^{-5} \text{ s}^{-1}$ on May 1 (Fig. 12b) to lower than $2.0 \times 10^{-5} \text{ s}^{-1}$ (Fig. 12c). When it arrives at the coastal ocean in the southeastern BOB and becomes phase locked with the surface vortex development, its intensity increases (Fig. 12d–f). Apparently this is quite favorable for the rapid development of the tropical storm. Figure 12 also shows the evolution of vorticity at 850 hPa (contour), which demonstrates the pronounced westward-propagating feature of the SCS positive vorticity center. In addition, a belt of positive vorticity exists across the southern BOB from May 1 to May 5. On May 5, when the westward-propagating upper-level divergence center arrives in the southeastern BOB, the local positive vorticity starts to increase rapidly (Fig. 12d) and accompanied by heavy rainfall of more than 40 mm day^{-1} (Fig. 9d). The strong convection and latent heating release result in further development of the cyclonic vorticity in the lower troposphere and divergence in the upper troposphere, and the upper and lower circulation systems become phase locked. The explosive development of the well-coupled system eventually leads to the genesis of the tropical storm over the southeastern BOB on May 5 (Fig. 12d), which experiences rapid intensification from May 7 to May 9 after the monsoon onset (Fig. 12e, f).

To further investigate how the convective heating over the SCS initiates the ASM onset vortex over the eastern BOB, cross sections of divergence and vorticity along the propagation pathway of the 200-hPa divergence center, as marked by the dashed blue lines in Fig. 12, are presented in Fig. 13. During the SCS heating, an upper-layer divergence center of greater than $4 \times 10^{-5} \text{ s}^{-1}$ appeared over the SCS (Fig. 13a). After the heating was shut down, the divergence center slowly propagated westward with its intensity maintained by $3 \times 10^{-5} \text{ s}^{-1}$ (Fig. 13b, c). Meanwhile, a lower-tropospheric positive vorticity system started to grow slowly over the tropical BOB. When the divergence center in the upper troposphere and the positive vorticity in the lower troposphere became phase locked on May 5 (Fig. 13d), the coupled system developed explosively: the vorticity in the lower layer exceeded $3 \times 10^{-5} \text{ s}^{-1}$ while the divergence in the upper layer enhanced. A remarkable vortex with an 850-hPa daily mean wind greater than 12 m s^{-1} was formed 1 day before the BOB monsoon onset on May 6. This coupled system moved westward—northward over the BOB ocean after the monsoon onset (Fig. 13e, f) and further intensified. By May 9, the storm reached its full development before it hit the western coast of Myanmar, with a surface vorticity of $4 \times 10^{-5} \text{ s}^{-1}$ and

Fig. 13 The same as Fig. 9 except that this figure shows the vertical cross section of divergence (shading, unit is 10^{-5} s^{-1}) and vertical vorticity (contour, unit is 10^{-5} s^{-1}) along the propagation direction of the 200-hPa divergence center as denoted by the dashed blue lines in Fig. 12



very well-developed upper-layer divergence of more than $3 \times 10^{-5} \text{ s}^{-1}$ (Fig. 13f).

The results from the sensitivity experiment agrees very well with the 2008 observations, which helps us understand the series of feedback loop and interaction between tropical cyclone development and monsoon onset. The severe weather over the BOB in spring of 2008 and the development of the strong tropical storm Nargis, is at least partly attributed to the development of the tropical storm Neoguri in mid-April over the SCS.

5 Conclusion and discussion

Based on observational analysis and numerical sensitivity experiments, interaction and feedback among tropical cyclone activities and the evolution of the SAH as well as their impact on summer monsoon onset over the SCS and BOB in 2008 are investigated in this study. The results show that atmospheric responses to strong convective latent heating over the SCS enhance the upper troposphere anticyclone and hence the SAH intensifies. Strong southward advection of vorticity to the east of the SAH and weak northward advection of vorticity to the west of SAH form a zonal asymmetric vorticity forcing with positive/

negative PV forcing to the east/west of the SAH. During the period with strong convective heating, the impact of the diabatic heating prevails over that of the asymmetric vorticity forcing and results in local enhancement of the SAH. At the time when the tropical cyclone decays and disappears, the convective diabatic heating disappears correspondingly. The asymmetric vorticity forcing becomes dominant and the SAH experiences an unstable development, which presents as a free westward-propagating Rossby wave. The upper-layer divergence center to the southwest of the SAH also propagates westward accordingly.

Previous study has demonstrated that a SST warm pool usually appears over central BOB in spring, mainly due to the thermal forcing of the Tibetan plateau and the distribution of land and sea in the tropics (Wu et al. 2012). This warm pool, combined with the persistent near-surface tropical westerly during this season, provides an ideal condition for tropical cyclogenesis. Cyclones usually develop under appropriate air-sea interaction conditions (Wu et al. 2011, 2012), or under unstable barotropic (Krishnamurti 1981, 1985; Mao and Wu 2011) or baroclinic large scale flows (Mak and Kao 1982). Such kind of conditions favorable for tropical cyclogenesis is common over BOB, whereas the vigorous development of the local

tropical cyclone to a deep convective MOV occurs only in certain years. Since more than 85 % of the atmospheric moisture resides in the lower atmosphere below 3 km, there must exist certain mechanism to pull the water vapor from the surface layer to the middle and upper troposphere in order to form monsoon cloud and precipitation. This study reveals that the upper layer pumping associated with the unstable development of the SAH and its phase-locking with the lower tropospheric cyclogenesis serve as such a mechanism. The unstable development of the SAH is triggered by the strong development of a tropical storm over the SCS. As a result, explosive cyclogenesis develops rapidly over the southern BOB, leading to generation of an intense tropical cyclone or vortex accompanied by severe weather and finally the ASM onset.

The experiment results obtained from this study was based on an atmospheric circulation model SAMIL. For comparison purpose, a more realistic air-sea coupled climate model with the same SAMIL as the atmospheric component has been used to conduct a similar set of experiments, in which the same diabatic heating as that in the HTG experiment was imposed over the SCS in the heating experiment. Results showed a similar consequence (figures not shown): in the heating experiment after the latent heating over the SCS withdrew, the generated SAH starts to propagate westward, with a strong divergence center gradually developed on its southwest. Due to the intensification of the upper tropospheric pumping, the existing positive vorticity zone in the southern BOB was then gradually organized and an apparent vortex was generated. On the contrary, such a cyclogenesis did not occur in the control experiment. These results presented in the experiments based on a climate model are in general the same as those based on an atmospheric general circulation model, and consolidate the conclusions obtained in this study.

To explore the universality of the conclusions just obtained, a composite analysis on the BOB monsoon onset based on the ECMWF Reanalysis data ERA-40 for the period 1979–2001 has been conducted, and the results, which will be published separately (Liu et al. 2013), prove that the upper tropospheric pumping in association with the unstable development of the SAH due to the convective latent heating over South Philippines prior to the BOB monsoon onset can be as strong as $8 \times 10^{-6} \text{ s}^{-1}$ in terms of climate- mean divergence; and it is such a strong pumping in the upper layer that contributes to the development of atmospheric ascent and cyclogenesis over the southern BOB and the monsoon onset.

This study focuses on one single mechanism concerning the coupling between the upper and lower tropospheric circulations and its contribution to the BOB tropical storm genesis. However, the BOB monsoon onset is affected not

only by local processes, i.e. sea surface conditions (Joseph 1990; Yang and Lau 1998), air-sea interactions (Wu et al. 2011, 2012), and barotropic and baroclinic instability, but also by the north–south thermal gradient (Li and Yanai 1996) and ENSO events, etc. However, the following questions are not answered yet about how the mechanism identified in this study is interwoven with other mechanisms and jointly contributes to the monsoon onset and how these mechanisms vary at different time scales to affect the monsoon variability, and deserve further studies.

Acknowledgments We thank the two anonymous reviewers for their constructive comments and suggestions. This study was jointly supported by the MOST Programme 2010CB950403 and 2012CB417203, CAS project XDA10010402 and NSF of China Projects 40925015 and 41275088.

References

- Bao Q, Liu YM, Shi JC, Wu GX (2010a) Comparisons of soil moisture datasets over the Tibetan Plateau and application to the simulation of Asia summer monsoon onset. *Adv Atm Sci* 27(2):303–314
- Bao Q, Wu GX, Liu YM et al (2010b) An introduction to the coupled model FGOALS1.1-s and its performance in East Asia. *Adv Atm Sci* 5:167–178
- Guo L, Liu YM (2008) The effects of diabatic heating on asymmetric instability and the Asian extreme climate events. *Meteor Atmos Phys* 100:195–206
- He JH, Wen M, Shi XH, Zhao QH (2002) Splitting and eastward withdrawal of the subtropical high belt during the onset of the South China Sea summer monsoon and their possible mechanism. *J Nanjing Univ (Nat Sci)* 38(3):318–330
- Hoskins BJ, McIntyre ME, Robertson AW (1985) On the use and significance of isentropic potential vorticity maps. *Quart J Roy Meteor Soc* 111:877–946
- Hsu CJ, Plumb RA (2000) Nonaxisymmetric thermally driven circulations and upper-tropospheric monsoon dynamics. *J Atmos Sci* 57:1255–1276
- Huffman GJ, Adler RF, Morrissey MM, Curtis S, Joyce R, McGavock B, Susskind J (2001) Global precipitation at one-degree daily resolution from multi-satellite observations. *J Hydrometeor* 2:36–50
- Huffman GJ, Adler RF, Bolvin DT et al (2007) The TRMM multi-satellite precipitation analysis: Quasi-global, multi-year, combined-sensor precipitation estimates at fine scale. *J Hydrometeor* 8:38–55
- Hurrell JW, Hack JJ, Shea D et al (2008) A new sea surface temperature and sea ice boundary dataset for the community atmosphere model. *J Climate* 21:5145–5153
- Joseph PV (1990) Warm pool over Indian Ocean and monsoon onset. *Trop Ocean Atmos Newslett* 53:1–5
- Kalnay E, Kanamitsu M, Kistler R, Collins W, Deaven D, Gandin L, Iredell M, Saha S, White G, Woollen J, Zhu Y, Leetmaa A, Reynolds B, Chelliah M, Ebisuzaki W, Higgins W, Janowiak J, Mo KC, Ropelewski C, Wang J, Jenne R, Joseph D (1996) The NCEP/NCAR 40-year reanalysis project. *Bull Am Met Soc* 77:437–471
- Kikuchi K, Wang B, Fudeyasu H (2009) Genesis of tropical cyclone Nargis revealed by multiple satellite observations. *Geophys Res Lett* 36:L06811. doi:10.1029/2009GL037296

- Krishnamurti TN (1981) Cooling of the Arabian Sea and the onset-vortex during 1979. Recent progress in equatorial oceanography: a report of the final meeting of SCOR Working Group 47 in Venice, Italy, pp 1–12 (Available from Nova University, Ocean Science Center, Dania, FL 33004)
- Krishnamurti TN (1985) Summer monsoon experiment—a review. *Mon Weather Rev* 113:1590–1626
- Krishnamurti TN, Ramanathan Y (1982) Sensitivity of the monsoon onset to differential heating. *J Atmos Sci* 39(6):1290–1306
- Krishnamurti TN, Ardanuy P, Ramanathan Y et al (1981) On the onset vortex of the summer monsoon. *Mon Weather Rev* 109(2):344–363
- Lau KM, Wu HT, Yang S (1998) Hydrologic processes associated with the first transition of the Asian summer monsoon: a pilot satellite study. *Bull Am Met Soc* 79(9):1871–1882
- Lau KM, Ding Y, Wang JT et al (2000) A report of the field operations and early results of the South China Sea Monsoon Experiment (SCSMEX). *Bull Am Met Soc* 81(6):1261–1270
- Li C, Yanai M (1996) The onset and interannual variability of the Asian summer monsoon in relation to land-sea thermal contrast. *J Clim* 9:358–375
- Li WW, Wang CZ, Wang DX, Yang L, Deng Y (2012) Modulation of low-latitude west wind on abnormal track and intensity of tropical cyclone Nargis (2008) in the Bay of Bengal. *Adv Atmos Sci* 29(2):407–421. doi:10.1007/s00376-011-0229-y
- Liu YM, Wu GX, Liu H, Liu P (2001) Condensation heating of the Asian summer monsoon and the subtropical anticyclones in the eastern hemisphere. *Clim Dyn* 17:327–338
- Liu YM, Chan JCL, Mao JY, Wu GX (2002) The role of Bay of Bengal convection in the onset of the 1998 South China Sea summer monsoon. *Mon Weather Rev* 130:2731–2744
- Liu YM, Hoskins BJ, Blackburn M (2007) Impacts of the Tibetan topography and thermal forcing over Asia in summer. *J Meteor Soc Jpn* 85B:1–19
- Liu BQ, He JH, Wang LJ (2012) On a possible mechanism for southern Asian convection influencing the South Asian High establishment during winter to summer transition. *J Trop Meteor* 18:473–484
- Liu B, Wu G, Mao J, He J (2013) Genesis of the South Asian High and its impact on the Asian Summer Monsoon Onset. *J Clim*. doi:10.1175/JCLI-D-12-00286.1
- Long XM, Wang SA, Shang XD, Chen RY, Wang DX (2010) Monitoring disastrous hydrometeorological environment related to typhoons around the Xisha Islands. *J Trop Oceanog* 29(6):29–33 (In Chinese with English abstract)
- Mak M, Kao CYJ (1982) An instability study of the onset-vortex of the southwest monsoon, 1979. *Tellus* 34:358–368
- Mao JY, Wu GX (2007) Interannual variability in the onset of the summer monsoon over eastern Bay of Bengal. *Theor Appl Climatol* 89:155–170
- Mao JY, Wu GX (2011) Barotropic process contributing to the formation and the growth of tropical cyclone Nargis. *Adv Atmos Sci* 28(3):1–9
- Mao JY, Wu GX, Liu YM (2002) Study on modal variation of subtropical high and its mechanism during seasonal transition, Part II: seasonal transition index over Asian monsoon region. *Acta Meteor Sinica* (in Chinese) 60(4):409–420
- Mao JY, Chan JCL, Wu GX (2004) Relationship between the onset of the South China Sea summer monsoon and the structure of the Asian subtropical anticyclone. *J Meteor Soc Jpn* 82(3):845–849
- McPhaden MJ, Foltz GR, Lee T et al (2009) Ocean-Atmosphere interactions during cyclone Nargis. *EOS* 90(7):53–60
- Tiedtke M (1989) A comprehensive mass flux scheme for cumulus parameterization in large-scale models. *Mon Weather Rev* 117:1779–1800
- Wang ZZ, Yu RC, Wang PF, and Wu GX (2005) The development of GOALS/LASG AGCM and its global climatological features in climate simulation. II—The increase of vertical resolution and its influences. *J Trop Meteorol* (in Chinese) 21(3):238–247
- Webster PJ, Yang S (1992) Monsoon and ENSO: selective systems. *Quart J Roy Meteor Soc* 118:877–926
- Wu GX, Liu HZH (1999) Complete form of vertical tendency and slantwise vorticity development. *Acta Meteor Sinica* (in Chinese) 57(1):1–15
- Wu GX, Zhang YS (1998) Tibetan Plateau forcing and the situating and timing of the Asian monsoon onset. *Mon Wea Rev* 126:913–927
- Wu GX, Chou JF, Liu YM, He JH (2004) Dynamics of the formation and variation of subtropical anticyclone. Science Press, Beijing 315 pp
- Wu GX, Guan Y, Wang TM, Liu YM, Yan JH, Mao JY (2011) Vortex genesis over the Bay of Bengal in spring and its role in the onset of the Asian summer monsoon. *Sci China Earth Sci* 54:1–9. doi:10.1007/s11430-010-4125-6
- Wu GX, Guan Y, Liu YM, Yan JH, Mao JY (2012) Air-sea interaction and formation of the Asian summer monsoon onset vortex over the Bay of Bengal. *Clim Dyn* 38:261–279. doi:10.1007/s00382-010-0978-9
- Xu J, Chan JCL (2001) First transition of the Asian summer monsoon in 1998 and the effect of the Tibet: tropical ocean thermal contrast. *J Meteor Soc Japan* 79:241–253
- Yan JH (2005) The onset and March of the Asia summer monsoon and the variation of subtropical high. Institute of Atmospheric Physics, Chinese Academy of Sciences (PhD thesis), 147 pp
- Yang S, Lau KM (1998) Influences of sea surface temperature and ground wetness on Asian summer monsoon. *J Clim* 11:3230–3246
- Yu H, Hu CH, Jiang LY (2007) Comparison of three tropical cyclone intensity datasets. *Acta Meteor Sinica* 21:121–128
- Zhang YS, Wu GX (1998) Diagnostic investigations of the mechanism responsible for the onset of the Asian summer monsoon and abrupt seasonal transitions over the northern hemisphere, Part I: periodic feature of the Asian monsoon onset. *Acta Meteor Sinica* 56:1–16
- Zhang YS, Wu GX (1999) Diagnostic investigations of the mechanism responsible for the onset of the Asian summer monsoon and abrupt seasonal transitions over the northern hemisphere, Part II: roles of the surface sensible heating over the Tibetan Plateau and its vicinity. *Acta Meteor Sinica* 57:56–73